JOURNAL OF APPLIED POLYMER SCIENCE VOL. 15, PP. 811–828 (1971)

A Rationale for the Preparation of Loeb-Sourirajan-Type Cellulose Acetate Membranes

H. STRATHMANN,* P. SCHEIBLE, and R. W. BAKER,†
Technische Hochschule, Aachen, Germany

Synopsis

An attempt has been made to rationalize the variables in the preparation procedure of Loeb-Sourirajan-type reverse-osmosis membranes. The quaternary phase diagram of the system cellulose acetate–acetone–formamide–water was determined and has proved a useful tool in the discussion of membrane structures and properties. A mechanism based on differences in the precipitation rate of the polymer during the membrane formation process has been suggested to explain the observed asymmetry in the membrane structure. The porosity of the membrane has been ascribed to the relative rates of water entering and solvent leaving the cast film. The effects of the casting solution composition, the evaporation time, the wash bath temperature, and the annealing procedure have been studied. X-Ray diffraction and electron microscopy were used to supplement flux and retention data of membranes made from a cellulose acetate–formamide–acetone casting solution.

INTRODUCTION

Since Reid and Breton[1] discovered that cellulose acetate membranes could be successfully used to desalt water, increasing attention has been paid to developing improved membranes for this process. A novel new preparation technique developed by Loeb and Sourirajan[2] has led to dramatically improved reverse-osmosis membranes. These membranes have an asymmetric structure consisting of a 0.2–0.5 μm thick, dense layer, supported by a 50–100 μm thick porous substructure.[3] This substructure has pores of 0.1–1.0 μm in diameter. It has little or no effect on the solvent permeability or solute retention. Its only function is to support the thin, dense skin layer which represents the actual membrane. Because the solvent permeability is inversely proportional to the permeation path length, it is desirable to make the barrier as thin as possible.

The original recipe and subsequent modifications for preparing asymmetric membranes are deeply rooted in empiricism; numerous literature references[4–8] give detailed descriptions of the membrane preparation technique. Yet no comprehensive theory has evolved to unify the various strategems of the art in terms of a basic mechanism. This paper is addressed to this task. From the variety of recipes for making Loeb-Sourira-

* Present address: Amicon Corporation, Lexington, Massachusetts 02173.
† Present address: Pharmetrics, Palo Alto, California 94304.

jan-type cellulose acetate membranes a set of four essential steps can be extracted:

1. A solution of polymer in an appropriate solvent or solvent mixture is cast in a thin film on a plate.
2. Some of the solvent is allowed to evaporate by exposing the film for a certain time to the air.
3. The film, still on the plate, is immersed and precipitated in a fluid (usually water) which is a nonsolvent for the polymer but is miscible with the polymer solvent.
4. The film is annealed in hot water.

Various mechanisms have been suggested for explaining the skin formation. They are summarized by Lonsdale.[9] It has generally been agreed that during the evaporation step, solvent is lost from the film surface and the polymer concentration in the surface layer is increased.[10] When the film is then immersed in the water bath, water rapidly diffuses into the interior, the water concentration soon exceeds the solubility of the polymer, and gelation then occurs. During the posttreatment or annealing step, the membrane shrinks and the porosity decreases.

Keilin[5] has treated the membrane formation process as a gelation phenomena consisting of the steps coacervation and polymer desolvation, followed by syneresis and capillary depletion. In the coacervation step, the polymer assumes a spherical droplet form which encapsulates most of the solvent. The encapsulated solvent forms the final membrane pores. As desolvation continues, the coacervated droplets come into contact and bond through the intermingling of polymer molecules from neighboring droplets. Syneresis and capillary depletion take place during the membrane-annealing step.

Keilin was particularly concerned with the effects of water and salts such as $ZnCl_2$ and $Mg(ClO_4)_2$ in casting solutions of cellulose acetate and acetone. He postulated that the superior membranes obtained from casting solutions containing these additives were due to the increased swelling of the membrane. The salts were thought to delay gelation by forming ionic complexes with the polymer which increased repulsion of the polymer aggregates. In addition, he postulated that the salts tend to attract osmotically water into the structure.

Kesting and Menfee[11] used a treatment similar to that of Keilin to explain the formation of the membrane. In addition, they explained the asymmetric structure by suggesting that interfacial forces and the surface-active properties of the polymer caused an increase in the concentration of polymer at the polymer–solution interface.

Bloch and co-workers[12,13] related the porosity of the membrane and the skin formation to the concentration of water required for precipitating the cellulose acetate from the casting solution and to the direction and magnitude of osmotic flows taking place during the leaching.

In the present study, the quaternary phase diagram of the system cellulose acetate–formamide–acetone–water has been determined and is used as a tool in discussing membranes obtained from various casting solution compositions. The formation mechanism of the asymmetric membrane structure has been discussed in terms of precipitation kinetics, analogous to crystallization from supersaturated solutions. The membrane-annealing procedure has been studied by x-ray diffraction. Electron photomicrographs have been used in conjunction with filtration tests to support the postulated membrane formation mechanism.

EXPERIMENTAL

Determination of Phase Diagram. The phase diagram was determined by preparing solutions of cellulose acetate–formamide–acetone and titrating water into these solutions until the first permanent turbidity was obtained. This indicated the boundary of the one-phase region. A further quantity of water was added and the two phases which formed were separated by filtration and were analyzed. The cellulose acetate content was determined from the weight after evaporation to dryness. The formamide and water concentrations were measured radiochemically with ^{14}C-labelled formamide and ^{3}H-labelled water using a liquid scintillation counter. The accuracy of the radiochemical analysis was within $\pm 5\%$. The acetone content was determined from a mass balance.

Membrane Preparation. The membranes used in this work were prepared from a formulation first used by Manjikian,[7,8] of Eastman cellulose acetate (39.8% acetyl content, ASTM viscosity 3), formamide, and acetone. Unless otherwise indicated, the casting solution composition was 25% by weight cellulose acetate, 45% by weight acetone, and 30% by weight formamide. The solution was prefiltered and centrifuged at 3000 g for 20 min before use. From this solution, films 0.1–1 mm thick were cast in a dust-free chamber onto a clean, polished glass plate. After an evaporation step of 0.5–2 min at room temperature, the films were immersed in an ice bath for 1 hr. The membranes were then removed from the plate and annealed for 0.5–3 min in water at 60°–90°C. The membranes were stored at 6°–8°C. Extreme care in filtering and centrifuging the casting solution and in maintaining a dust-free atmosphere was necessary to avoid erratic and generally lower salt rejections.

Membrane Filtration Tests. Water and salt fluxes were measured in a stirred batch cell with a 1% NaCl solution at an applied pressure of 100 atm. Feed and bleed concentrations were determined by conductivity measurements to an accuracy of ±1%. The batch cell and the test stand are described elsewhere.[14] The salt rejection of the membranes is expressed in per cent of the bulk solution concentration. Product flux data are given in gallons per square feet and day (gsfd).

X-Ray and Electron Microscopy Studies. The degree of crystallinity of the membranes was studied by x-ray diffraction. Samples of the membranes

were sealed in thin-walled capillaries and x-ray photographs were taken. Exposure times were between 6 and 10 hr. A Zeiss electron microscope was used to study chromium-shadowed carbon replicas of the membrane surfaces.

Membrane Composition. The cellulose acetate content of the final membranes was determined by measuring the per cent weight loss on drying membrane samples in a vacuum oven.

RESULTS AND DISCUSSION

The Phase Diagram

Figure 1 shows the composite phase diagram of the system cellulose acetate–formamide–acetone–water. The upper triangular surface of the prism describes the system cellulose acetate–acetone–water. In the lower triangular surface, acetone has been replaced by formamide. All points within the prism represent mixtures of all four components. Points in the diagram indicated by circles represent a mixture of solid and a liquid phase, the compositions of which are indicated by triangles and squares, respectively. The corresponding three points are connected by tie lines. Within the prism, solid phase compositions are enriched in acetone relative to the liquid phase compositions with which they are tied. The diagram also shows cellulose acetate to be slightly more soluble in an acetone–water mixture than in a formamide–water mixture. Both results are not surprising in view of the solubility parameter of cellulose acetate (11.5–12.5), which is closer to that of acetone (9.9) than that of formamide (19.2).

The section through the quaternary phase diagram at the acetone-to-formamide ratio of 6:4 is shown in Figure 2. Manjikian found this ratio of acetone to formamide in the casting solution to give the best desalination membranes. Although the two-phase region in the quaternary system changes slightly with the acetone-to-formamide ratio, Figure 2 will be used to discuss the membrane formation procedure, since small changes in the two-phase region are irrelevant for this general discussion. The mixture of acetone and formamide is taken as one component and represented by the term "solvent." When the membrane is precipitated by immersing the film into a water bath, the mixture changes as water is added and solvent is lost from casting solution composition to final membrane composition represented by A and D, respectively. Note that D represents the composition of the total membrane as determined by analysis and does not distinguish between a skin formed at the upper membrane surface and the porous substructure. Point D represents a composition averaged over the total membrane cross section. The composition of the skin might well differ from this value; in cases where an evaporation step is involved in the membrane-making procedure, the skin composition is certainly different from that in the substructure. Although it would be preferable to know the composition of the skin alone, this information is difficult to obtain experimentally. In any case, the composition of the skin is likely to

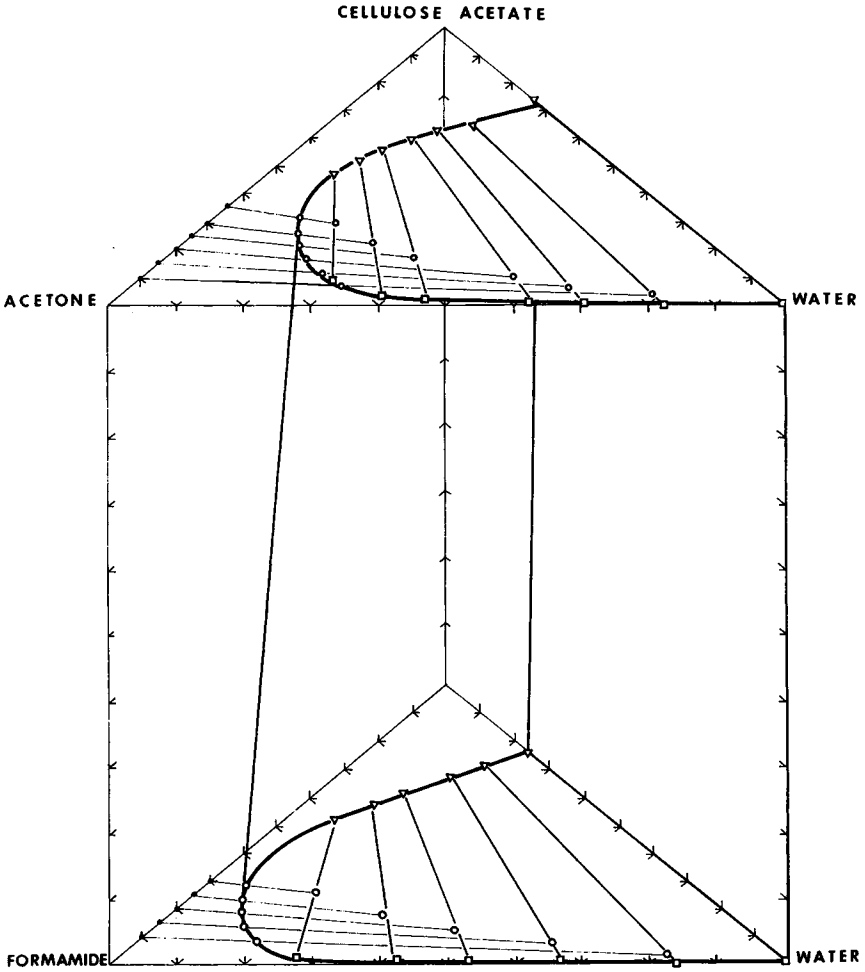

Fig. 1. Phase diagram of the system cellulose acetate–formamide–acetone–water.

parallel that of the substructure (and hence, total membrane) as confirmed by the excellent agreement between bulk composition and transport properties. The composition of the final membrane given by point D in Figure 2 represents a mixture of a solid phase S, which comprises the membrane pore walls, and a liquid phase L within the membrane pores. The composition of the two phases is given by the position of D on the line SL.

Though D gives the overall ratio of solid to liquid phase, it does not give any information about the dispersion of the two phases or the detailed path from A to D, which is determined by the kinetics of precipitation. The cellulose acetate content, that is, the overall porosity, may gradually change during the entire precipitation procedure. The path may follow the line ABD in Figure 2, but the total porosity may also be set as soon as the composition reaches the two-phase region. In this case, the path would follow

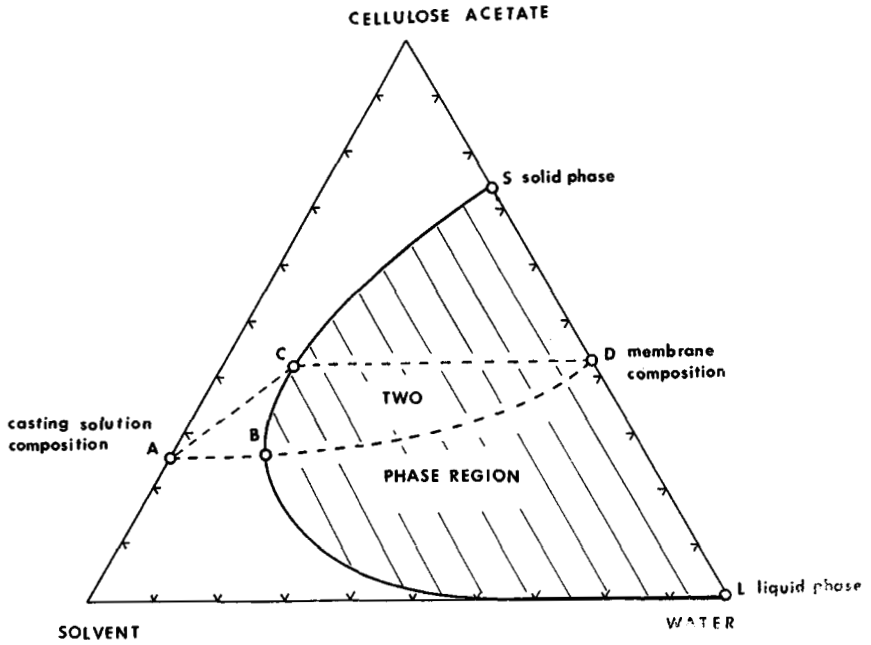

Fig. 2. A section of the quaternary phase diagram shown in Fig. 1. The term "solvent" represents a mixture of 40 wt-% formamide and 60 wt-% acetone.

the line ACD where the portion of the path through the two-phase region is parallel to the solvent–water line. However, the specific path through the phase diagram is not relevant to the following discussion, and the lines connecting the casting solution composition with those of the final membrane in Figures 2, 3, 4, and 6 do not necessarily represent the true path through the phase diagram during the membrane precipitation.

Membrane Casting Solution Composition

The general effect of the membrane casting solution composition on the properties of the membrane is shown in Figure 3.

The overall porosity of a membrane is determined by two parameters: (1) the cellulose acetate content of the casting solution and (2) the relative rates at which water enters and solvent leaves the casting solution (i.e., the precipitation path in the phase diagram). Figure 3 shows the path of precipitation of several casting solution compositions. Path AE represents a membrane formed when during the precipitation step water enters the film faster than the solvent leaves. This leads to highly porous membranes. Path AF is the precipitation path followed when solvent leaves and water enters at the same rate. Path AD is followed when the solvent leaves the film faster than water enters. The result is a dense membrane. The effect of all successful additives and modifications of the original cellulose acetate–acetone casting solution (e.g., formamide, $ZnCl_2$, $Mg(ClO_4)_2$,

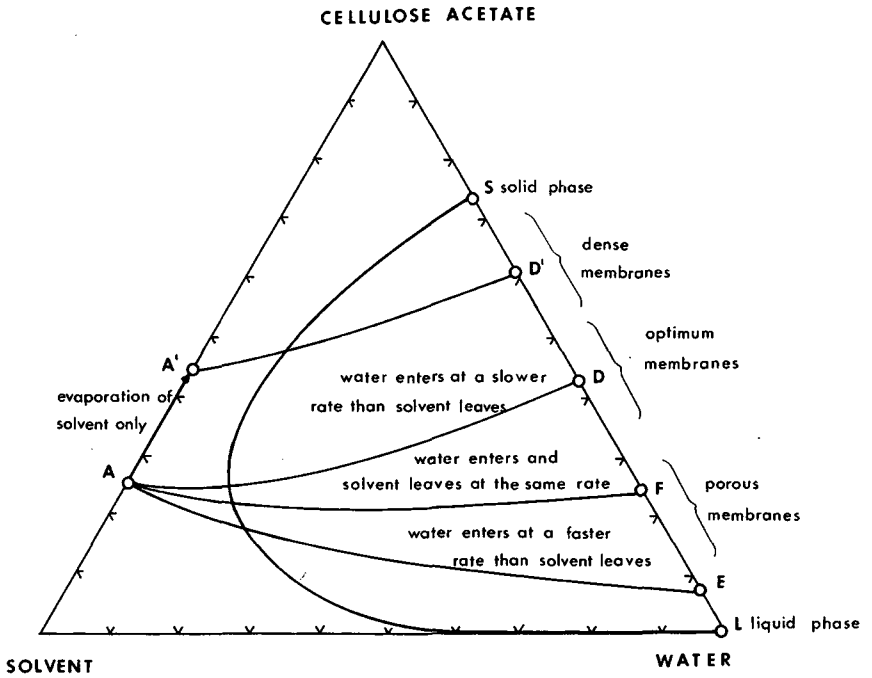

Fig. 3. Phase diagram of the system cellulose acetate–solvent–water, showing the precipitation paths at various relative rates of water diffusing in and solvent diffusing out of the casting solution.

etc.) is to adjust the relative rates of solvent loss and water gain during the membrane precipitation so as to produce membranes which fall in an optimum porosity range of 0.5 to 0.7. Although this porosity range can be obtained by adjusting the cellulose acetate content of the casting solution, this is impractical since the viscosity range is too broad to form coherent membranes.

Formamide is one of the most successfully used additives in cellulose acetate–acetone casting solutions. According to Manjikian,[7] the optimum casting solution is 25% cellulose acetate, 45% acetone, and 30% formamide. A membrane obtained from this casting solution is represented by the point D in Figures 2 and 3.

The effect of the formamide concentration in the casting solution on the overall membrane porosity is shown in Figure 4. As the concentration of formamide in the casting solution of a constant cellulose acetate content is increased, the membrane porosity also increases. In Figure 5, the water and salt fluxes at 100 atm pressure are expressed as a function of formamide content in the casting solution. At low formamide concentrations, the salt and water fluxes both increase and their ratio is nearly constant, i.e., the rejection is constant. However, at formamide concentrations in excess of about 30%, the salt rejection decreases drastically.

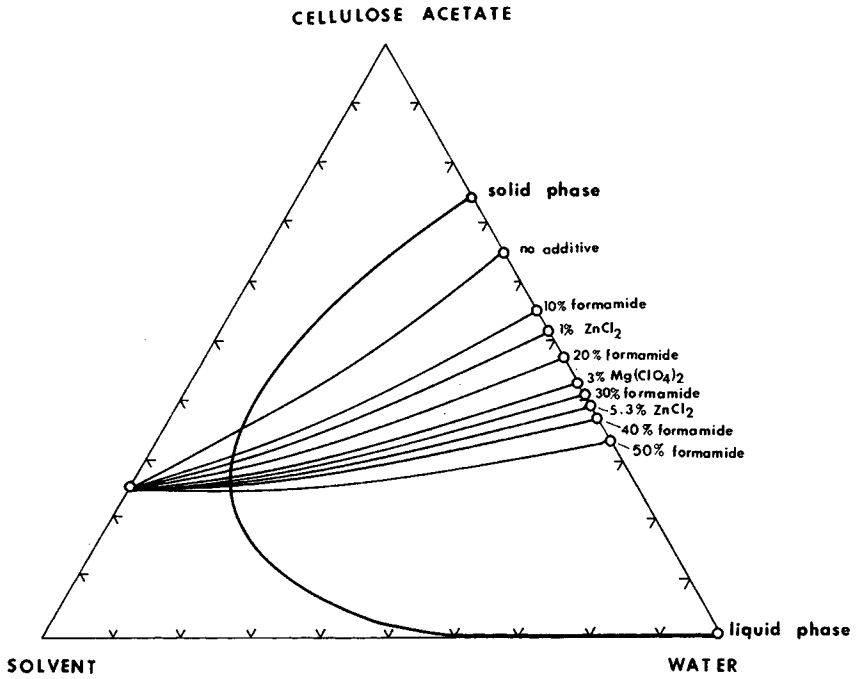

Fig. 4. Phase diagram of the system cellulose acetate–solvent–water, showing the effect of various additives on the precipitation path.

The above results taken with those of other investigators support the proposition that membrane porosity alone, and not the method of achieving it (whether by additives or cellulose acetate concentration), is the determinant of transport properties. For example, Keilin prepared membranes of about the same degree of porosity as those studied in this work using $ZnCl_2$, and $Mg(ClO_4)_2$ instead of formamide as additives to the membrane casting solution. His results, shown also in Figure 4, illustrate the pronounced change in the membrane porosity that a small quantity of added salt can cause. Figure 4 also shows that three membranes made from entirely different casting solution compositions (viz., (1) 25% cellulose acetate, 30% formamide, and 45% acetone; (2) 25% cellulose acetate, 72% acetone, and 3% $Mg(ClO_4)_2$; (3) 25% cellulose acetate, 69.7% acetone, and 5.3% $ZnCl_2$) all have essentially identical properties, viz., porosities between 0.58 and 0.62, salt rejections between 98% and 99%, and water fluxes between 15 and 25 gsfd at 100 atm hydrostatic pressure. Membranes having a lower porosity than the above may be prepared from casting solutions which contain, in addition to cellulose acetate and acetone, either 10% formamide or 1% $ZnCl_2$. These membranes have essentially identical porosities of 0.45 and also approximately the same transport properties (98%–99% rejection and 2–5 gsfd at 100 atm hydrostatic pressure). It is believed that the main parameter determining the membrane

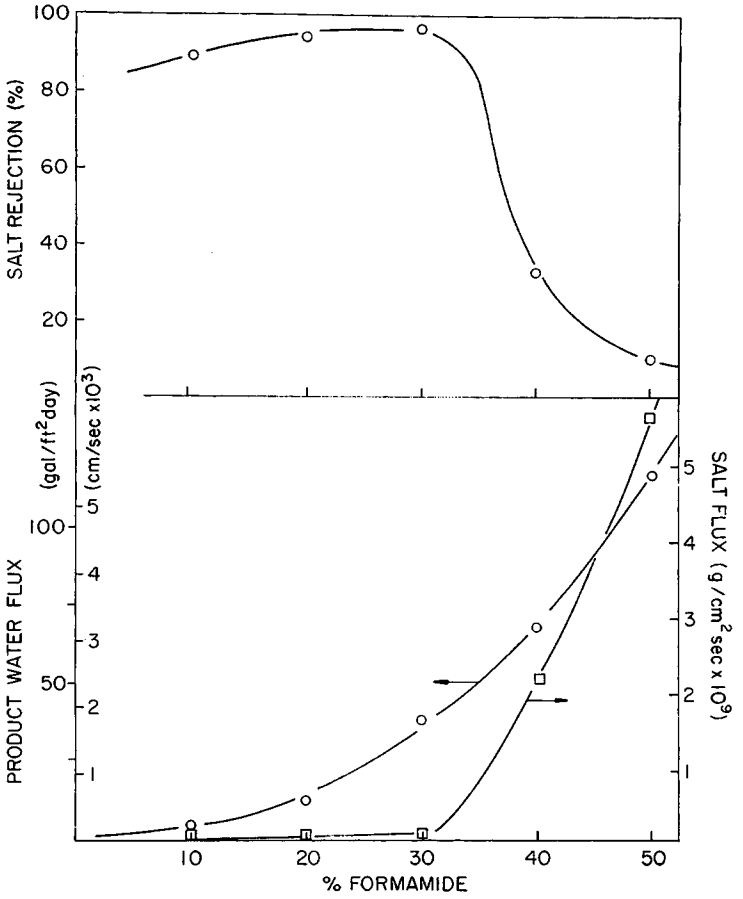

Fig. 5. Retention and flux data for membranes prepared from a casting solution with 25% cellulose acetate and varying proportions of acetone and formamide. (The membranes had an evaporation time of 1 min at 25°C and a heat treatment of 2 min at 75°C.)

transport properties is the overall porosity, which should be between 0.55 and 0.65 for high-flux, high-salt-rejection (>98%) membranes, irrespective of the casting solution composition. Membranes having a porosity less than 0.55 have low water fluxes, but the salt rejection is generally greater than 98%. Membranes having a porosity higher than 0.65 in general have very high water fluxes in excess of 50 gsfd but low salt rejections of 30%–50%, as indicated in Figure 3. The probable action of casting solution additives is to decrease the difference in the chemical potential of the acetone and increase the difference in the chemical potential of the water between the casting solution and the wash bath. This causes a decrease in the rate at which acetone leaves and an increase in the rate at which water enters the casting solution.

Water was one of the earliest additives incorporated in cellulose acetate–acetone casting solutions. Figure 6 shows results published for several

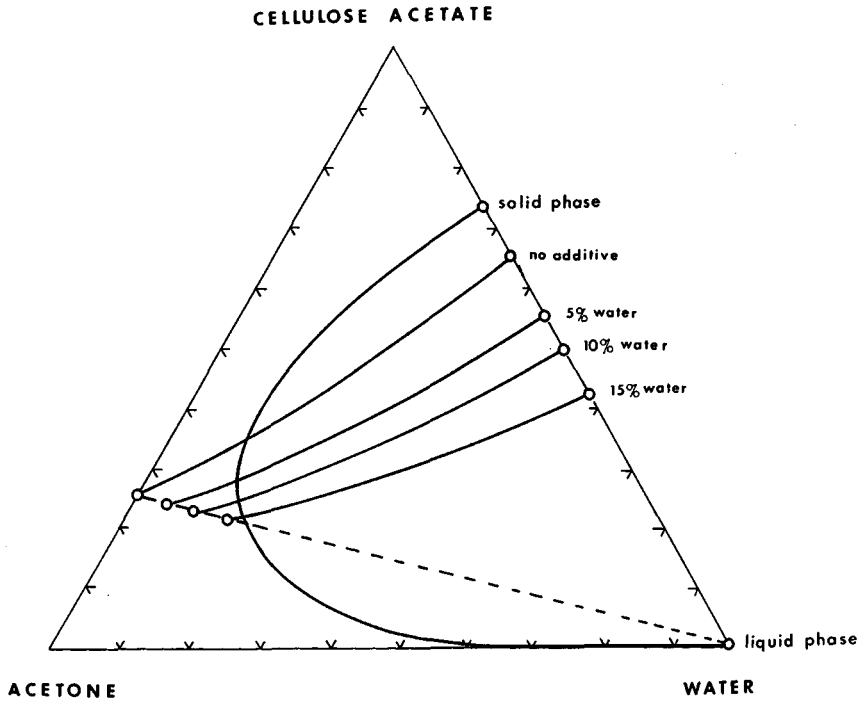

Fig. 6. Effect of small quantities of water in a cellulose–acetate–acetone casting solution on final membrane porosity.

casting solutions containing increasing concentrations of water.[5] The phase diagram approach allows these results to be easily explained. The casting solution with 15% water already contains so much water that only a small amount need diffuse in before the gelation line is reached and the membrane sets. This results in a more porous membrane. For casting solutions containing 5% and 10% water, however, a much larger volume of water must diffuse in prior to gelation; while this occurs, a substantial amount of acetone diffuses out. In this case, the final membranes have lower porosity and consequently lower water fluxes.

Formation of Asymmetric Membranes

Although the phase diagram gives a general relation between the casting solution composition and the overall porosity, i.e., the ratio of solid to liquid phase in the final membrane, it does not give any information about the dispersion of the two phases, which is also a determining factor for the final membrane pore size. Furthermore, it does not explain the asymmetric structure of the Loeb-Sourirajan-type membrane. It is believed that this asymmetry can be rationalized in terms of the membrane precipitation kinetics. Polymer precipitation can be treated by analogy to crystallization from supersaturated solutions. The relationship between nucleation, nuclei growth, and degree of supersaturation in crystallization has

been discussed by Volmer[15] and others.[16,17] This relationship is shown in a general way in Figure 7, where the rate of precipitation is plotted against the nucleus size for different degrees of supersaturation. The intercept of these curves with the abscissa gives the critical nucleus size, above which a spontaneously formed nucleus will grow. With increasing supersaturation, the critical nucleus size decreases. Since the density of spontaneously formed nuclei is a function of nucleus size, at high supersaturations the rate of precipitation is higher than at low supersaturations and, more important, the precipitate is more finely dispersed. This is a general observation of analytical and preparative chemistry.

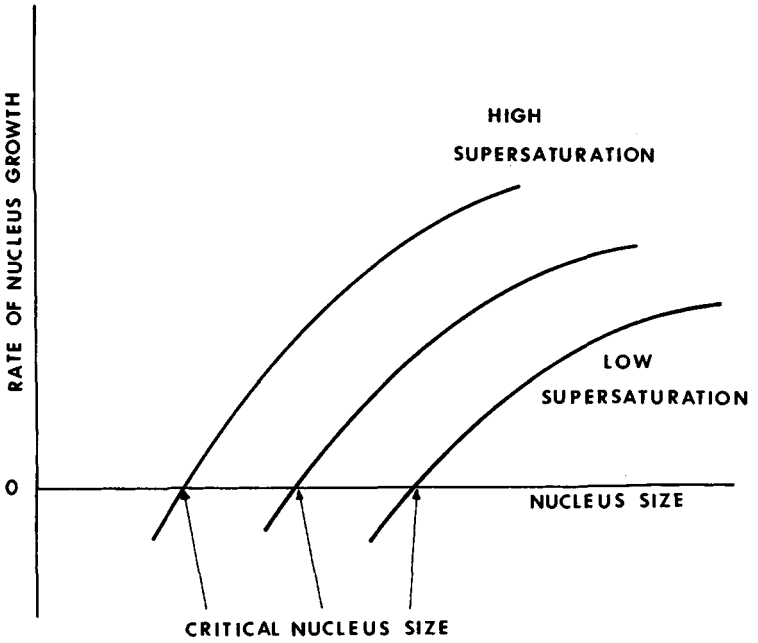

Fig. 7. Schematic diagram showing the relationship between rate of precipitation, critical nucleus size, and degree of supersaturation during a precipitation process.

This general concept of precipitation can be transferred to the membrane formation. At the outermost surface, where the cast membrane solution is in direct contact with the water of the precipitation bath, the degree of supersaturation is extremely high and the density of nuclei and the rate of their growth is also high. This results in a finely dispersed structure which corresponds to the final membrane skin. As the precipitation front moves further into the film, its composition becomes progressively richer in solvent, and water has to diffuse through the already formed membrane skin into the precipitation zone. The degree of supersaturation is significantly lowered and the precipitate becomes increasingly coarser. In this way, the average pore size increases from top to bottom of the membrane.

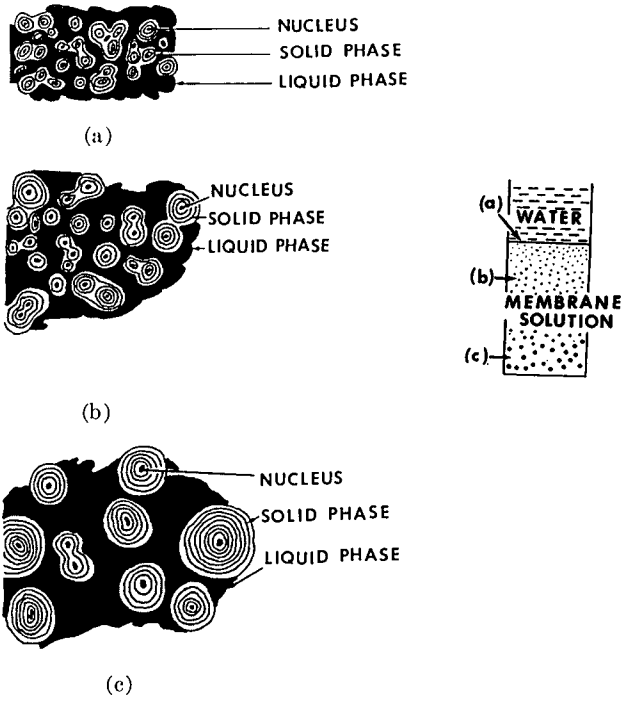

Fig. 8. Schematic diagram of polymer precipitation at different points through membrane cross section. (a) High supersaturation at the membrane surface; many nuclei, rapid growth. (b) Lower supersaturation; fewer nuclei, less rapid growth. (c) Low supersaturation; few nuclei, slow growth.

Figure 8 shows a schematic diagram of the precipitation process at various supersaturations; at the membrane surface (a), just below the membrane surface (b), and at the membrane bottom (c). This figure illustrates the way in which the average pore size changes drastically from the top to the bottom of the membrane. The process can be reproduced on a larger scale with a drop of polymer casting solution between two microscope slides. If water is injected next to the casting solution, the process of precipitation in the surface and sublayers can be easily followed with an optical microscope. This mechanism would predict that the thickness of the membrane skin, and with it the membrane transport properties, should be more or less independent of the drawdown thickness of the casting solution.

In Figure 9, the product flux obtained at 100 atm hydrostatic pressure with distilled water is plotted versus the membrane thickness. It shows that the permeability of these membranes is indeed independent of drawdown thickness. Furthermore, this membrane formation mechanism predicts that a membrane precipitated slowly at a low supersaturation should have very large pores, and if the degree of supersaturation is kept constant during the entire precipitation procedure, a more or less asymmetric structure without a skin layer should be obtained. This has been achieved by

precipitating the membrane in a water- and solvent-saturated atmosphere of a glove box at 25°C. The rate of precipitation is then determined by the diffusion rate of water from the vapor phase into the casting solution. A very porous, symmetric membrane structure was obtained. Figure 10

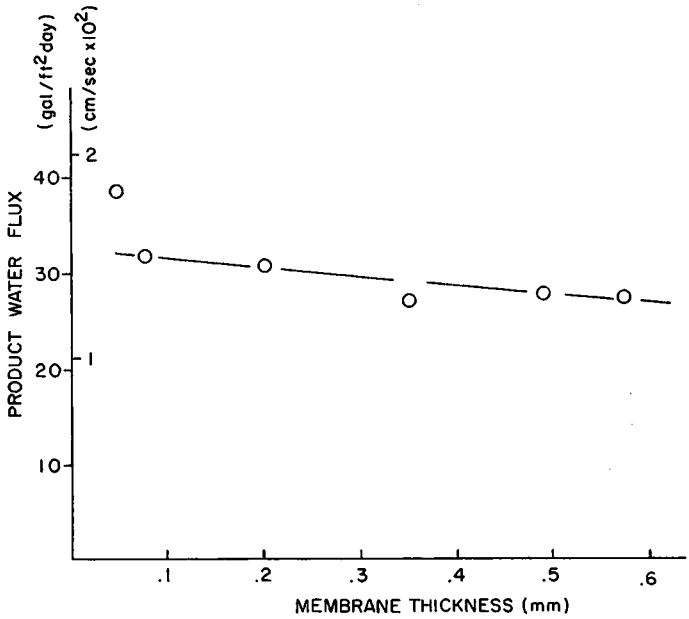

Fig. 9. Effect of drawdown thickness on membrane flux.

shows electron photomicrograph of the upper and lower surface of this membrane, while Figure 11 shows the surfaces of an asymmetric membrane made from the same casting solution by the regular precipitation procedure described in the experimental section.

The Evaporation Step

The evaporation step in the membrane preparation procedure is used to make more retentive membranes. During this step, solvent is lost mainly from the cast film surface, thus increasing its solids content. This is shown schematically in Figure 3. During the evaporation step, the casting solution composition changes from a composition represented by point A to one represented by A′. When this solution is precipitated, a considerably denser membrane, represented by point D′ in this diagram, is obtained. It is believed that the increase of the cellulose acetate concentration at the membrane surface due to solvent evaporation, in combination with the precipitation kinetics, is the main reason for the formation of the dense and highly salt-rejecting skin of the Loeb-type membrane. Figure 12 shows the effect of evaporation time on membrane salt retention determined at 100 atm hydrostatic pressure with a 1% NaCl solution. The drop in re-

jection at 1–2 min evaporation time is probably the result of preferential evaporation of acetone causing the formamide concentration to exceed 35% which, as can be seen from Figure 5, produces membranes having low salt rejections.

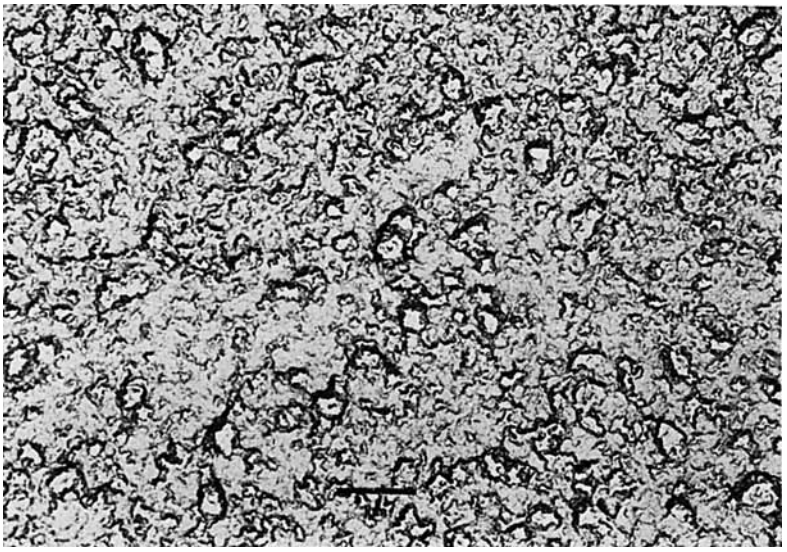

(a)

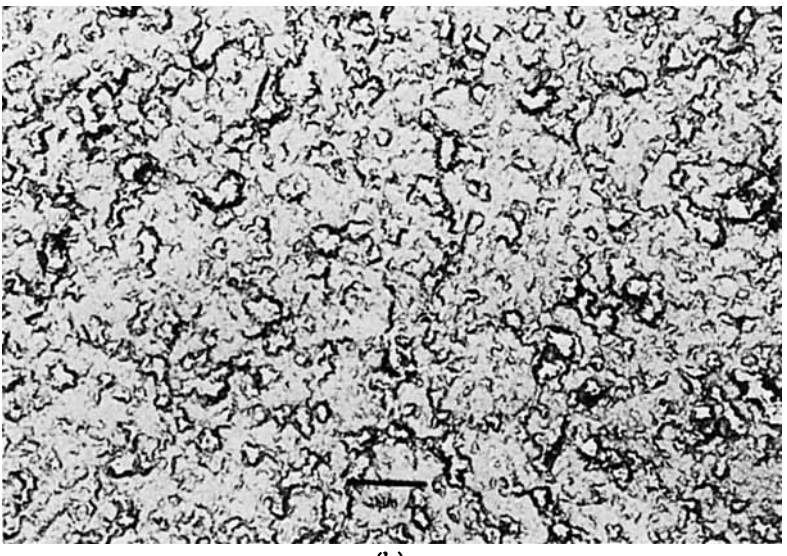

(b)

Fig. 10. Electron micrographs of top (a) and bottom (b) surfaces of a symmetric membrane prepared by precipitation in a solvent- and water-saturated atmosphere (magnification 13,000:1).

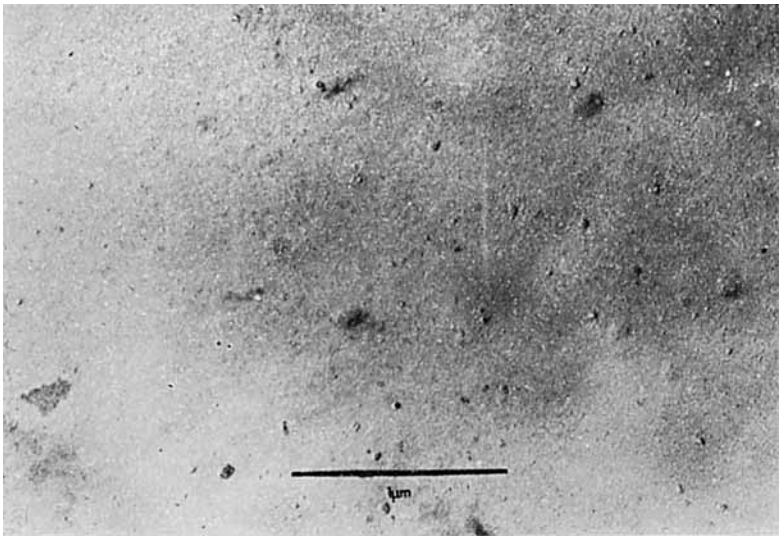

(a)

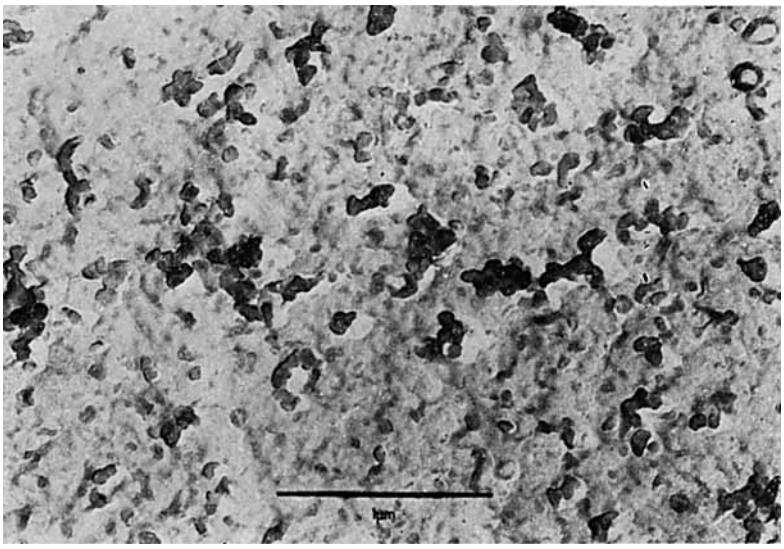

(b)

Fig. 11. Electron micrographs of top (a) and bottom (b) surfaces of an asymmetric membrane (magnification 37,000:1).

The Membrane-Annealing Step

Annealed membranes have a lower water flux and a higher salt retention than unannealed membranes. Figure 13 shows the water flux and retention obtained at 100 atm pressure with a 1% NaCl solution for a series of membranes annealed for 1 min at different temperatures. The reduction

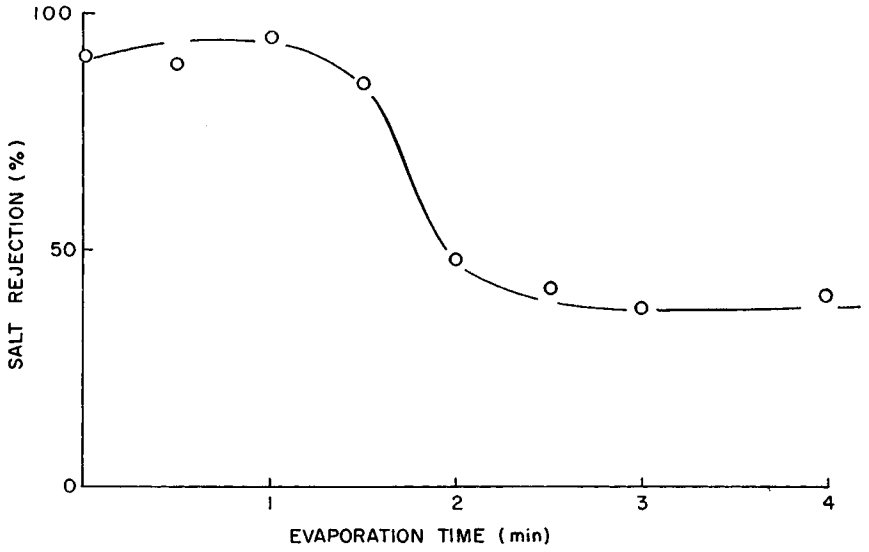

Fig. 12. Effect of evaporation time at 25°C on salt rejection of membrane cast from 25 wt-% cellulose acetate, 30 wt-% formamide, and 45 wt-% acetone. Membranes were annealed for 2 min at 75°C.

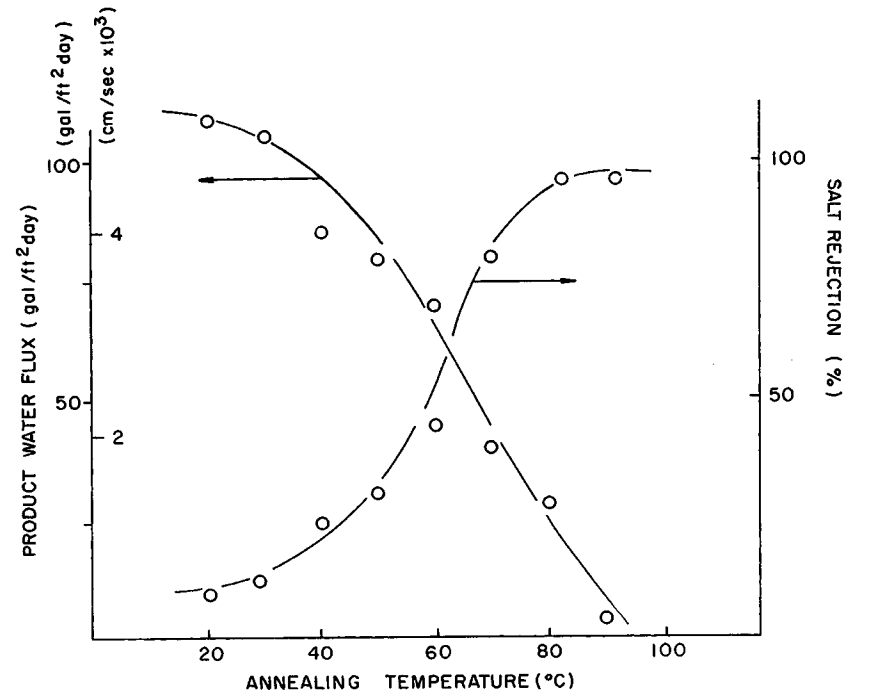

Fig. 13. Effect of annealing temperature on the retention and flux of membranes cast from 25% cellulose acetate, 30% formamide, and 45% acetone. Evaporation time was 2 min at 25°C.

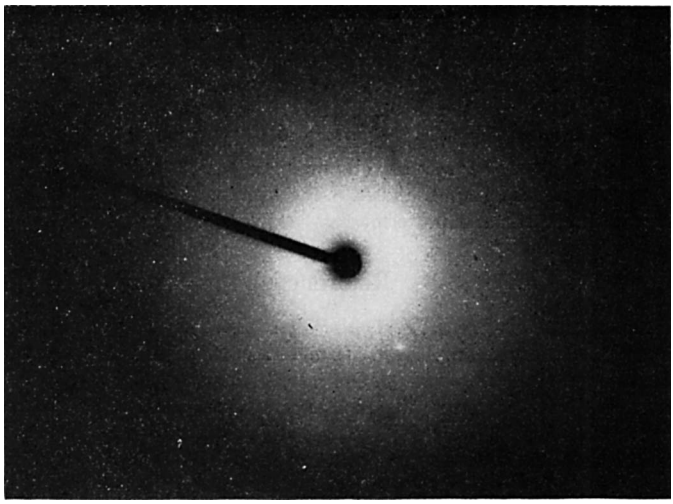

(a)

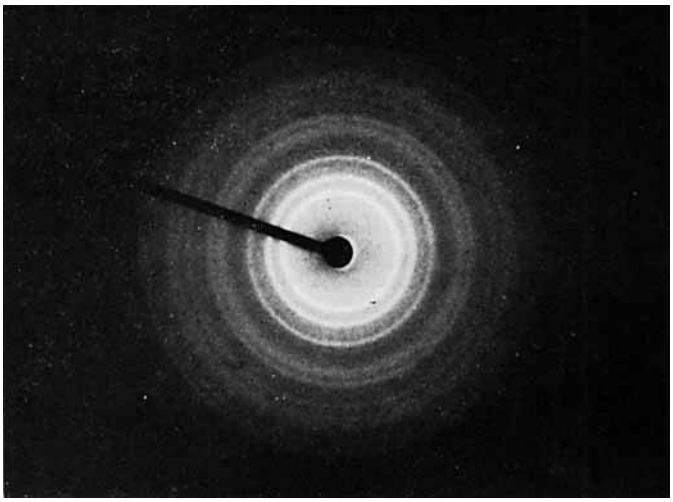

(b)

Fig. 14. X-Ray photographs of an unannealed membrane (a) and a membrane annealed for 5 min at 100°C (b). Note the marked increase in crystallinity after annealing.

in pore sizes accompanying the shrinkage which takes place on annealing is probably partially responsible for these effects. An additional cause is the restricted polymer mobility accompanying the increased degree of crystallinity. Thus, while dry cellulose acetate has a glass transition temperature over 100°C,[18] in the plasticized wet form it may have a considerably lower value. The x-ray photographs shown in Figure 14 confirm the increase in crystallinity upon annealing. A membrane after 5 min annealing at 100°C is much more crystalline than an unannealed membrane. The increased crystallinity markedly reduces the freedom of movement of the polymer

chains, causing the hydrated salt to be excluded to a greater degree than the smaller water molecules. The rejection coefficient of the membrane therefore increases.

We are indebted to the Technische Hochschule, Institut für Physik und Chemie, Aachen, Germany, where the bulk of this work was completed. We are also indebted to R. W. Hauslein, M. J. Lysaght, and A. S. Michaels for many enlightening discussions during the preparation of this manuscript.

References

1. C. E. Reid and E. T. Breton, *J. Appl. Polym. Sci.*, **1**, 33 (1959).
2. S. Loeb and S. Sourirajan, *Advan. Chem. Ser.*, **38**, 117 (1962).
3. R. L. Reiley, S. Merten, and J. O. Gardner, *Desalination*, **1**, 30 (1966).
4. B. Keilin, Office of Saline Water Research and Development Report No. 84, U. S. Government Printing Office, Washington, D. C., January 1964.
5. B. Keilin, Office of Saline Water Research and Development Report No. 117, U. S. Government Printing Office, Washington, D. C., August 1964.
6. S. Loeb, in *Desalination by Reverse Osmosis*, U. Merten, Ed., M.I.T. Press, Cambridge, Mass., 1966.
7. S. Manjikian, *Ind. Eng. Chem., Prod. Res. Develop.*, **6**, 23 (1967).
8. S. Manjikian, S. Loeb, and J. W. McCutchan, Proceedings of First International Desalination Symposium, Washington, D.C., 1965, Vol. 2, pp. 159–173.
9. H. K. Lonsdale, in *Desalination by Reverse Osmosis*, U. Merten, Ed., M.I.T. Press, Cambridge, Mass., 1966.
10. W. Banks and A. Sharples, *J. Appl. Chem.*, **16**, 28 (1966).
11. R. E. Kesting and A. Menfee, *Kolloid-Z. Z. Polym.*, **230**, 341 (1968).
12. R. Bloch and M. A. Frommer, *Desalination*, **7**, 259 (1969).
13. M. A. Frommer, I. Feiner, O. Kedem, and R. Bloch, *Desalination*, **7**, 393 (1970).
14. H. Strathmann and P. Scheible, in press.
15. M. Volmer, *Kinetik der Phasenbildung*, Steinkopff, Dresden and Leipzig, 1939.
16. J. N. Stranski and R. Kaischew, *Z. Phys. Chem.*, (B)**26**, 317 (1934).
17. U. F. Franck, *Werkst. Korros.*, **5**, 367 (1963).
18. J. H. Daane and R. E. Barker, Jr., J. Polym. Sci., **2**, 343, (1964).

Received October 22, 1970
Revised December 4, 1970